

# The Control of the Nitrogen Inversion in Alkyl-Substituted Diaziridines<sup>‡</sup>

O. Trapp,<sup>[a]</sup> V. Schurig,<sup>\*[b]</sup> and R. G. Kostyanovsky<sup>\*[c]</sup>

**Abstract:** For the first time the nitrogen inversion barriers in 3,3-unsubstituted *trans*-diaziridines, such as 1,2-di-*tert*-butyldiaziridine (**1**) and 1,2-di-*n*-butyldiaziridine (**2**) were determined. Enantioselective stopped-flow multidimensional gas chromatography was used to investigate the enantiomerization barrier of **1** between 126.2 and 171.0 °C ( $\Delta G_{\text{gas}}^{\ddagger}(150.7^{\circ}\text{C}) = 135.8 \pm 0.2 \text{ kJ mol}^{-1}$ ,  $\Delta H_{\text{gas}}^{\ddagger} = 116.1 \pm 2.5 \text{ kJ mol}^{-1}$ ,  $\Delta S_{\text{gas}}^{\ddagger} = -46 \pm 2 \text{ J K}^{-1} \text{ mol}^{-1}$ ). The separation of the

enantiomers has been achieved in presence of the chiral stationary phase (CSP) Chirasil- $\beta$ -Dex with a high separation factor ( $\alpha = 1.44$  at 80 °C). In a complementary approach, the enantiomerization barriers of 1,2-di-*tert*-butyldiaziridine (**1**), 1,2-di-*n*-butyldiaziridine

(**2**), 1-*n*-butyl-3,3-dimethyldiaziridine (**3**), and 1,2,3,3-tetramethyldiaziridine (**4**) were determined for comparison by enantioselective dynamic chromatography (DGC) and computer simulation of the dynamic elution profiles.

The enantiomerization barrier of **2** was shown to be the highest among the nonsterically hindered diaziridines studied so far, whereas **1** exhibited the highest value found for strained nitrogen-containing rings, that is, aziridines, diaziridines and oxaziridines.

**Keywords:** chirality • enantiomerization barrier • gas chromatography • N heterocycles • steric hindrance

## Introduction

In 1967, Mannschreck et al. discovered that nitrogen inversion in diaziridines is hindered on the NMR<sup>[1a]</sup> time scale. They later determined the inversion barriers (108–113 kJ mol<sup>-1</sup>) by means of an NMR method.<sup>[1b]</sup> The first optically active diaziridines were reported in 1974,<sup>[2a]</sup> and their absolute configurations were established by X-ray diffraction analysis.<sup>[2c,g,m]</sup> Chiroptical properties<sup>[2q,r]</sup> and configurational stability were studied by racemization kinetics.<sup>[2]</sup> In 1979, Mannschreck et al. applied chiral chromatography

to the optical resolution of diaziridines and also measured the inversion barriers by racemization kinetics.<sup>[1c,f]</sup> In all known examples, the inversion barriers of diaziridines did not exceed 117 kJ mol<sup>-1</sup> (see review in ref. [3]). However, there are possibilities to increase the inversion barriers in diaziridines.

First, the inversion barriers in 3,3-unsubstituted diaziridines were not measured until now and an increase of the inversion barrier could be expected on account of the lack of 1,2-nonbonding interactions that destabilize the ground state. This is supported by the nitrogen inversion barrier in 1-methylaziridine being 7.1 kJ mol<sup>-1</sup> higher than those in 1,2,2-trimethylaziridine.<sup>[3]</sup>

Next, there is an opportunity for steric hindrance of the inversion in diaziridines at the cost of a destabilization of the inversion transition state.<sup>[4]</sup> Indeed, in 1-alkylaziridines the transfer from methyl to *tert*-butyl substituents results in a decrease of the barrier by 8.4 kJ mol<sup>-1</sup>,<sup>[3]</sup> whereas in 1,2-di-*tert*-butyl-substituted pentacyclic hydrazines the inversion barrier is the highest found so far for heterocycles of this kind.<sup>[4]</sup>

In the present study, the enantiomerization barriers of 1,2-di-*tert*-butyldiaziridine (**1**),<sup>[2]</sup> 1,2-di-*n*-butyldiaziridine (**2**),<sup>[1g,2r]</sup> 1-*n*-butyl-3,3-dimethyldiaziridine (**3**),<sup>[1c,e]</sup> and 1,2,3,3-tetramethyldiaziridine (**4**)<sup>[1c,e]</sup> were elucidated by two contemporary enantioselective gas chromatographic methods (Scheme 1).

[a] Dr. O. Trapp

Stanford University, Department of Chemistry  
Stanford, California 94305-5080 (USA)  
Fax: (+1) 650-725-0259  
E-mail: trapp@stanford.edu

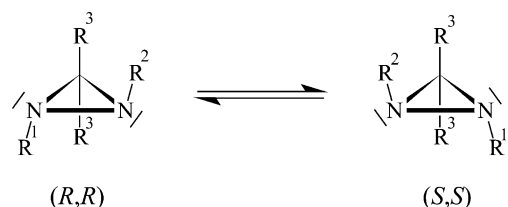
[b] Prof. Dr. V. Schurig

University of Tübingen, Institute of Organic Chemistry  
Auf der Morgenstelle 18, 72076 Tübingen (Germany)  
Fax: (+49) 7071-29-5538  
E-mail: volker.schurig@uni-tuebingen.de

[c] Prof. Dr. R. G. Kostyanovsky

N. N. Semenov Institute of Chemical Physics, Russian Academy of Sciences  
Kosygina street 4, 119991 Moscow, Russian Federation (Russia)  
Fax: (+7) 095-938-2156  
E-mail: kost@chph.ras.ru

[<sup>‡</sup>] Asymmetric Nitrogen, Part 90. For Part 89, see: V. Yu. Torbeev, K. A. Lyssenko, O. N. Kharybin, M. Yu. Antipin, R. G. Kostyanovsky, *J. Phys. Chem. B*, **2003**, *107*, 13523–13531.



Scheme 1. Enantiomerization of 1,2-di-*tert*-butyldiaziridine (**1**,  $R^1 = R^2 = \text{Me}_3\text{C}$ ,  $R^3 = \text{H}$ ), 1,2-di-*n*-butyldiaziridine (**2**,  $R^1 = R^2 = \text{Me}(\text{CH}_2)_3$ ,  $R^3 = \text{H}$ ), 1-*n*-butyl-3,3-dimethyldiaziridine (**3**,  $R^1 = \text{Me}(\text{CH}_2)_3$ ,  $R^2 = \text{H}$ ,  $R^3 = \text{Me}$ ), and 1,2,3,3-tetramethyldiaziridine (**4**,  $R^1 = R^2 = R^3 = \text{Me}$ ).

## Results and Discussion

The enantiomers of **1**, **2**, **3**, and **4** were separated by enantioselective gas chromatography in the presence of the chiral stationary phase (CSP) Chirasil- $\beta$ -Dex<sup>[5]</sup> with a considerable separation factor ( $\alpha$ ) for **1** ( $\alpha(80^\circ\text{C}) = 1.44$ ; Figure 1), whereas the  $\alpha$  value of **2** was only 1.05 under the same chromatographic conditions as given in Figure 1, the  $\alpha$  value for

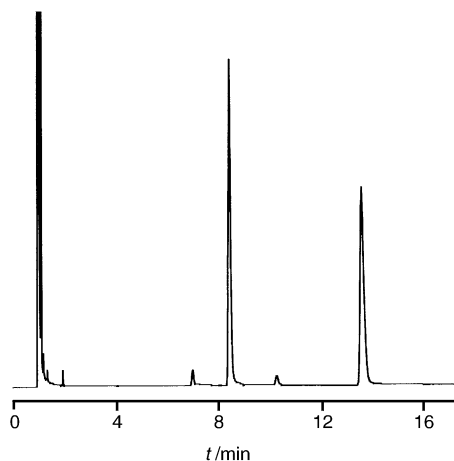


Figure 1. Separation of the enantiomers of 1,2-di-*tert*-butyldiaziridine (**1**) at  $80^\circ\text{C}$  in presence of the CSP Chirasil- $\beta$ -Dex (separation factor  $\alpha = 1.44$ ). Chromatographic conditions: 25 m Chirasil- $\beta$ -Dex (0.25 mm i.d., film thickness 0.5  $\mu\text{m}$ ). Carrier gas:  $\text{H}_2$ , column head pressure 0.25 bar.

**3** was 1.08 at  $70^\circ\text{C}$  (50 m Chirasil- $\beta$ -Dex, 0.25 mm i.d., film thickness 0.3  $\mu\text{m}$ , carrier gas:  $\text{H}_2$ , column head pressure 0.95 bar) and for **4**  $\alpha = 1.09$  at  $65^\circ\text{C}$  (50 m Chirasil- $\beta$ -Dex, 0.25 mm i.d., film thickness 0.3  $\mu\text{m}$ , carrier gas:  $\text{H}_2$ , column head pressure 0.5 bar).

To quantify the enantiomerization barrier of **1** in the inert gas phase, the enantioselective stopped-flow multidimensional gas chromatographic method (sfMDGC),<sup>[6]</sup> which was recently developed for the determination of very high enantiomerization (inversion) barriers, was applied to determine the enantiomerization rate constants  $k_1^{\text{gas}}$ , as described in the Experimental Section. The sfMDGC experiment can easily be carried out at different temperatures (Table 1), yielding the activation parameters  $\Delta H_{\text{gas}}^\ddagger$  and  $\Delta S_{\text{gas}}^\ddagger$ . The enantiomerization barrier ( $\Delta G_{\text{gas}}^\ddagger = 135.8 \pm 0.2 \text{ kJ mol}^{-1}$  at  $150.7^\circ\text{C}$ ) of **1**

Table 1. Results of the temperature-dependent sfMDGC experiments of the enantiomerization of 1,2-di-*tert*-butyldiaziridine (**1**). Where *e.r.* denotes the de novo enantiomeric ratio found after enantiomerization at temperature  $T$  for  $t$  minutes. Mean values and standard deviations were calculated from at least three experiments at each temperature.

$T$ [ $^\circ\text{C}$ ]	$t$ [min]	<i>e.r.</i>	$k_1^{\text{gas}}$ [ $\text{s}^{-1}$ ]	$\Delta G_{\text{gas}}^\ddagger$ [ $\text{kJ mol}^{-1}$ ]
126.2	15.0	53.8	$2.08 \times 10^{-5}$	$134.6 \pm 0.3$
138.2	21.0	12.0	$6.78 \times 10^{-5}$	$134.7 \pm 0.6$
150.7	20.3	5.4	$1.63 \times 10^{-4}$	$135.8 \pm 0.2$
162.0	12.3	3.4	$4.20 \times 10^{-4}$	$136.1 \pm 0.2$
171.0	10.0	2.2	$8.17 \times 10^{-4}$	$136.5 \pm 0.1$

represents the highest value found for nitrogen inversion in a three-membered ring compound.

The mean values of  $\ln(k_1^{\text{gas}}/T)$  were plotted as a function of  $T^{-1}$  according to the Eyring equation. By regression analysis (agreement factor  $r = 0.999$ , residual standard deviation  $s_y = 0.031$ )  $\Delta H_{\text{gas}}^\ddagger$  was found to be  $116.1 \pm 2.5 \text{ kJ mol}^{-1}$  and  $\Delta S_{\text{gas}}^\ddagger = -46 \pm 2 \text{ J K}^{-1} \text{ mol}^{-1}$  (Figure 2).

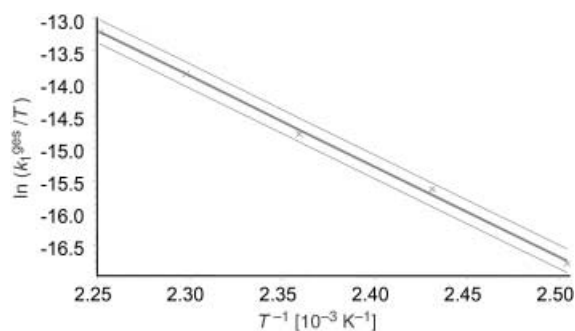


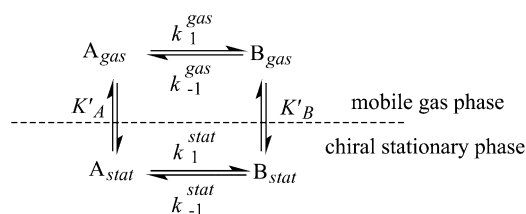
Figure 2. Eyring plot for the determination of the activation parameters  $\Delta H^\ddagger$  and  $\Delta S^\ddagger$  of 1,2-di-*tert*-butyldiaziridine (**1**) from the sfMDGC experiment. The upper and lower curves represent the error bands of the linear regression with a level of confidence of 95%.

In a complementary approach the enantiomerization barrier of **1** was also determined by enantioselective dynamic gas chromatography (DGC).<sup>[7]</sup> Dynamic chromatographic experiments require only nanomolar amounts of the unresolved stereoisomers (enantiomers). This also applies to the previously mentioned enantioselective sfMDGC. However, the prerequisite of dynamic chromatography is the quantitative on-column separation of the stereoisomers by a stereoselective stationary phase.

The elution profile of interconverting enantiomers in an enantioselective dynamic chromatographic experiment is characterized by plateau formation between the first enantiomer (eluted with peak tailing) and the second enantiomer (eluted with peak fronting). To evaluate the rate constants by computer simulation of elution profiles in dynamic chromatography, two basic models can be employed: i) the theoretical plate model<sup>[8]</sup> or ii) the stochastic model.<sup>[9]</sup> Recently, a mathematical function was derived to calculate the enantiomerization barriers directly.<sup>[10]</sup> The barrier of enantiomerization  $\Delta G^\ddagger$  of interconverting enantiomers is obtained as

a mean of the apparent enantiomerization rate constants  $k_1^{\text{app}}$  and  $k_{-1}^{\text{app}}$ .

The apparent rate constants represent a weighted mean of the rate constants in the gas phase  $k_1^{\text{gas}}$  (vide supra;  $k_{-1}^{\text{gas}}$  is equal for enantiomerization) and the different rate constants in the chiral stationary phase (CSP)  $k_1^{\text{stat}}$  and  $k_{-1}^{\text{stat}}$  (Scheme 2 and Equations (1a) and (1b) with the retention factor  $k' = (t_R - t_M)/t_M$ ).



Scheme 2. Equilibria of interconverting enantiomers on a single gas-chromatographic theoretical plate. A denotes the first eluted enantiomer, B denotes the second eluted enantiomer,  $k$  represents the rate constant and  $K'$  represents the distribution constant of the equilibrium between the mobile gas phase and the chiral stationary phase.

$$k_1^{\text{app}} = \frac{1}{1 + K'_A} k_1^{\text{gas}} + \frac{K'_A}{1 + K'_A} k_1^{\text{stat}} \quad (1a)$$

$$k_{-1}^{\text{app}} = \frac{1}{1 + K'_B} k_{-1}^{\text{gas}} + \frac{K'_B}{1 + K'_B} k_{-1}^{\text{stat}} \quad (1b)$$

The forward and backward rate constants in the chiral stationary phase are distinct, namely,  $k_1^{\text{stat}} > k_{-1}^{\text{stat}}$  because the enantiomers A and B have a different thermodynamic free Gibbs energy ( $-\Delta_{B,A}\Delta G$ ) in the presence of the chiral stationary phase ( $K'_B > K'_A$ ). The apparent rate constants themselves are varied until the simulated chromatogram coincides with the experimental chromatogram.

The elution profiles of the temperature-dependent enantioselective dynamic chromatographic experiments of **1** show a distinct plateau formation (110 and 119.7°C) and peak tailing of the first eluted enantiomer and peak fronting of the second eluted enantiomer (127–140°C) as the temperature increases between 100.0–140.0°C (Figure 3).

Selected experimental values of the enantioselective DGC experiments and the corresponding rate constants obtained by computer simulation with ChromWin<sup>[11]</sup> are given in Table 2. For the computer simulation, only elution profiles between 110.0 and 140.0°C were considered (28 experi-

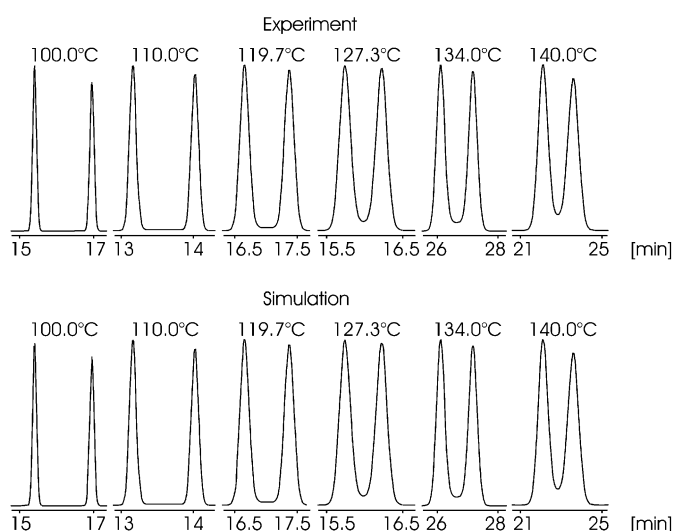


Figure 3. Chromatograms from the temperature-dependent DGC experiment for 1,2-di-*tert*-butyl diaziridine (**1**). Chromatographic conditions: 50 m Chirasil- $\beta$ -Dex<sup>5</sup> (0.25 mm i.d., film thickness 0.3  $\mu\text{m}$ ). Carrier gas: H<sub>2</sub>. Top: experimental chromatograms. Bottom: simulated elution profiles (ChromWin, SM+, method: “find enantiomerization barrier II”).

ments) because there was no plateau formation at lower temperatures.

For the evaluation of the activation parameters in the presence of the CSP Chirasil- $\beta$ -Dex,<sup>[5]</sup> the reaction rate constants of the enantiomerization process in the stationary phase were calculated according to Equations (1). The mean values of  $\ln(k_1^{\text{stat}}/T)$  were plotted as a function of  $T^{-1}$  according to the Eyring equation. By regression analysis (agreement factor  $r = 0.982$ , residual standard deviation  $s_y = 0.073$ )  $\Delta H_{\text{stat}}^{\ddagger}$  was found to be  $113.0 \pm 2.0 \text{ kJ mol}^{-1}$  and  $\Delta S_{\text{stat}}^{\ddagger} = -44 \pm 5 \text{ J K}^{-1} \text{ mol}^{-1}$ .

As evident from the values obtained by sfMDGC and DGC, the enantiomerization barriers  $\Delta G^{\ddagger}$  and activation parameters  $\Delta H^{\ddagger}$  and  $\Delta S^{\ddagger}$  of **1** agree very well.

In an effort to compare the enantiomerization barrier of **1** with structurally similar compounds, **2**, **3**, and **4** were synthesized and the enantiomerization barriers were investigated by enantioselective DGC. The elution profiles of the temperature-dependent enantioselective dynamic chromatographic experiments of **2**, **3** and **4** show plateau formation and peak broadening (peak tailing of the first eluted enantiomer and peak fronting of the second eluted enantiomer) as the temperature increases between 80.0 and 115.0°C for **2** (Figure 4a), 70.0°C and 110.0°C for **3** (Figure 4b) and 65.0°C and 92.3°C for **4** (Figure 4c).

Selected experimental values of the enantioselective DGC experiments and the corresponding rate constants obtained by computer simulation with ChromWin<sup>[11]</sup> are given in Table 3 for **2**, in Table 4 for **3** and in Table 5 for **4**. For the computer-assisted evaluation of the elution profiles, 21 experiments were considered for **2**,

Table 2. Selected experimental data from the temperature-dependent dynamic gas chromatographic experiment and rate constants of the enantiomerization of 1,2-di-*tert*-butyl diaziridine (**1**) in the presence of CSP Chirasil- $\beta$ -Dex.

$T$ [°C]	$t_M$ [min]	$t_R^A$ [min]	$t_R^B$ [min]	$w_A$ [s]	$w_B$ [s]	$h_{\text{plateau}}$ [%]	$k_1^{\text{app}}$ [ $10^{-3} \text{ s}^{-1}$ ]	$\Delta G_{\text{app}}^{\ddagger}$ [kJ mol <sup>-1</sup> ]
110.0	7.6	13.2	14.1	6.7	7.0	0.1	0.48	131.5
119.7	10.9	16.5	17.3	11.5	11.8	0.8	1.10	132.1
127.3	11.1	15.7	16.2	10.1	10.2	5.2	2.00	132.8
134.0	17.9	26.1	27.2	19.3	19.9	4.9	3.70	133.0
140.0	13.4	22.1	23.6	33.6	37.0	10.9	5.50	133.6

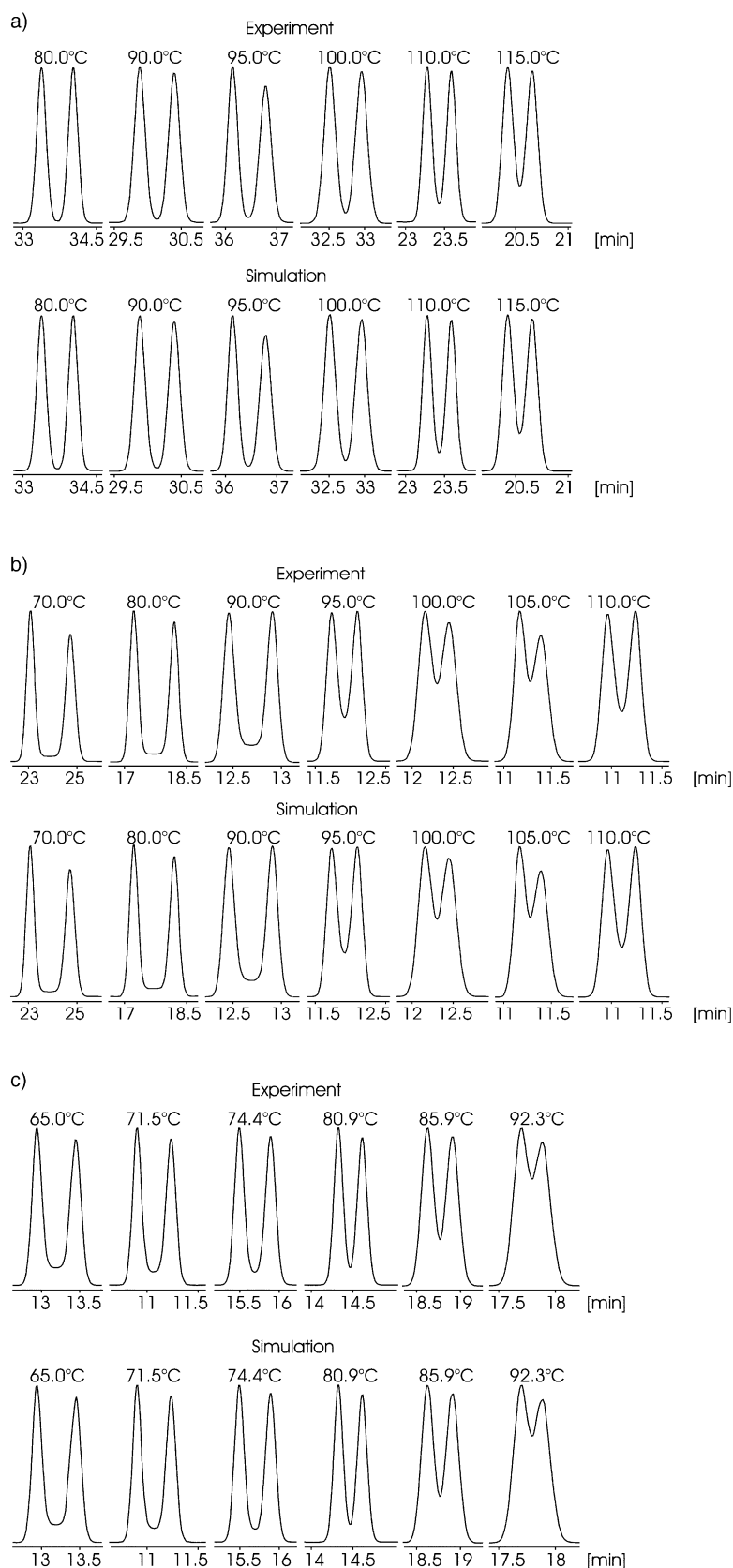


Figure 4. Chromatograms from the temperature-dependent DGC experiments of a) 1,2-dibutyldiaziridine (**2**), b) 1-butyl-3,3-dimethyldiaziridine (**3**), and c) 1,2,3,3-tetramethyldiaziridine (**4**). Chromatographic conditions: 50 m Chirasil- $\beta$ -Dex (0.25 mm i.d., film thickness 0.3  $\mu$ m). Carrier gas: H<sub>2</sub>. Top: experimental chromatograms. Bottom: simulated elution profiles (ChromWin, SM+, method: "finding enantiomerization barrier II")

25 experiments for **3** and 28 experiments for **4**.

To evaluate the activation parameters of **2**, **3** and **4**, the mean values of  $\ln(k_1^{\text{app}}/T)$  were plotted as a function of  $T^{-1}$  according to the Eyring equation. A regression analysis was used to obtain the activation enthalpies  $\Delta H^{\ddagger}_{\text{app}}$  and activation entropies  $\Delta S^{\ddagger}_{\text{app}}$  of **2** (agreement factor  $r = 0.998$ , residual standard deviation  $s_y = 0.089$ ), **3** ( $r = 0.9920$ ,  $s_y = 0.1024$ ) and **4** ( $r = 0.9905$ ,  $s_y = 0.1307$ ).

The activation parameters  $\Delta G^{\ddagger}$ ,  $\Delta H^{\ddagger}$ , and  $\Delta S^{\ddagger}$  of the compounds investigated here are summarized in Table 6. In contrast to tertiary amines and aziridines, where the barrier of nitrogen inversion decreases with increasing size of the substituents on the nitrogen atom as the pyramidal conformation is destabilized by steric interaction of bulky substituents,<sup>[3]</sup> the nitrogen inversion barrier in diaziridines increases with increasing size of the substituents.<sup>[3]</sup> Our experimentally determined enantiomerization barriers  $\Delta G^{\ddagger}$  corroborate the expected tendency: 1-*n*-butyl-3,3-dimethyldiaziridine (**3**) < 1,2,3,3-tetramethyldiaziridine (**4**) < 1,2-di-*n*-butyldiaziridine (**2**) < 1,2-di-*tert*-butyldiaziridine (**1**, Table 6).<sup>[1]</sup>

A comparison of the enantiomerization barriers of **1** ( $\Delta G^{\ddagger}_{\text{app}} = 132.5 \text{ kJ mol}^{-1}$ ,  $\Delta G^{\ddagger}_{\text{gas}} = 133.3 \text{ kJ mol}^{-1}$  and  $\Delta G^{\ddagger}_{\text{stat}} = 129.4 \text{ kJ mol}^{-1}$ ) and **2** ( $\Delta G^{\ddagger}_{\text{app}} = 125.2 \text{ kJ mol}^{-1}$ ) at an elevated temperature (150.7 °C) reveals a significant increase in the barrier for sterically hindered *tert*-butyl substituted diaziridine **1**.

The low activation enthalpies  $\Delta H^{\ddagger}$  and highly negative activation entropies  $\Delta S^{\ddagger}$ , particularly for **3** and **4**, can be attributed to steric and electronic effects of the twofold nitrogen inversion via a monoplanar transition state or may be considered as evidence for a dissociative mechanism of the

Table 3. Selected experimental data from the temperature-dependent dynamic gas chromatographic experiment and rate constants of the enantiomerization of 1,2-di-*n*-butyldiaziridine (**2**) in presence of the CSP Chiral- $\beta$ -Dex.

$T$ [°C]	$t_M$ [min]	$t_R^A$ [min]	$t_R^B$ [min]	$w_A$ [s]	$w_B$ [s]	$h_{\text{plateau}}$ [%]	$k_1^{\text{app}}$ [10 <sup>-5</sup> s <sup>-1</sup> ]	$\Delta G_{\text{app}}^{\ddagger}$ [kJ mol <sup>-1</sup> ]
80.0	3.4	33.4	34.0	13.5	13.3	1.0	0.30	122.3
90.0	4.6	29.9	30.4	11.3	11.8	2.0	0.65	123.5
95.0	5.6	36.2	36.8	13.5	15.6	3.2	1.24	123.3
100.0	7.3	32.5	33.0	11.9	12.4	6.5	1.36	124.7
110.0	7.2	23.3	23.6	8.3	8.5	11.7	5.29	123.8
115.0	7.3	20.4	20.6	7.2	7.6	23.8	10.50	123.3

Table 4. Selected experimental data from the temperature-dependent dynamic gas chromatographic experiment and rate constants of the enantiomerization of 1-*n*-butyl-3,3-dimethyldiaziridine (**3**) in presence of the CSP Chiral- $\beta$ -Dex.

$T$ [°C]	$t_M$ [min]	$t_R^A$ [min]	$t_R^B$ [min]	$w_A$ [s]	$w_B$ [s]	$h_{\text{plateau}}$ [%]	$k_1^{\text{app}}$ [10 <sup>-5</sup> s <sup>-1</sup> ]	$\Delta G_{\text{app}}^{\ddagger}$ [kJ mol <sup>-1</sup> ]
70.0	3.1	23.2	24.9	24.8	29.5	3.2	4.70	110.90
80.0	3.4	17.3	18.2	14.2	15.4	5.2	9.87	112.04
90.0	3.4	12.3	12.8	12.6	14.0	16.4	20.14	113.14
100.0	4.5	12.2	12.5	11.1	12.2	52.0	30.87	115.03
105.0	4.6	11.2	11.4	7.8	10.0	63.3	43.12	115.55
110.0	4.1	10.9	11.2	8.5	8.3	33.3	45.50	116.95

Table 5. Selected experimental data from the temperature-dependent dynamic gas chromatographic experiment and rate constants of the enantiomerization of 1,2,3,3-tetramethyldiaziridine (**4**) in presence of the CSP Chiral- $\beta$ -Dex.

$T$ [°C]	$t_M$ [min]	$t_R^A$ [min]	$t_R^B$ [min]	$w_A$ [s]	$w_B$ [s]	$h_{\text{plateau}}$ [%]	$k_1^{\text{app}}$ [10 <sup>-5</sup> s <sup>-1</sup> ]	$\Delta G_{\text{app}}^{\ddagger}$ [kJ mol <sup>-1</sup> ]
65.0	6.6	12.9	13.5	15.6	18.2	15.8	2.43	111.1
71.5	6.5	10.9	11.2	8.2	9.6	7.4	3.50	112.2
74.4	9.9	14.3	14.6	10.8	13.5	49.0	4.54	112.5
80.9	12.5	19.5	19.9	14.9	19.0	60.2	9.79	112.4
85.9	12.6	18.4	18.7	13.0	19.1	83.9	12.25	113.3
92.3	12.8	17.7	17.9	11.9	16.7	90.0	25.31	113.2

Table 6. Summary of the activation parameters for the enantiomerization of 1,2-di-*tert*-butyldiaziridine (**1**), 1,2-di-*n*-butyldiaziridine (**2**), 1-*n*-butyl-3,3-dimethyldiaziridine (**3**) and 1,2,3,3-tetramethyldiaziridine (**4**).

Compound	sfMDGC			DGC		
	$\Delta G_{298\text{K}}^{\ddagger}$ [kJ mol <sup>-1</sup> ]	$\Delta H^{\ddagger}$ [kJ mol <sup>-1</sup> ]	$\Delta S^{\ddagger}$ [JK <sup>-1</sup> mol <sup>-1</sup> ]	$\Delta G_{298\text{K}}^{\ddagger}$ [kJ mol <sup>-1</sup> ]	$\Delta H^{\ddagger}$ [kJ mol <sup>-1</sup> ]	$\Delta S^{\ddagger}$ [JK <sup>-1</sup> mol <sup>-1</sup> ]
<b>1</b>	129.8 ± 1.3 <sup>[a]</sup>	116.1 ± 2.5 <sup>[a]</sup>	-46 ± 2 <sup>[a]</sup>	126.1 ± 1.2 <sup>[b]</sup>	113.0 ± 2.0 <sup>[b]</sup>	-44 ± 5 <sup>[b]</sup>
<b>2</b>	--	--	--	124.0 ± 0.8 <sup>[c]</sup>	118.9 ± 1.0 <sup>[c]</sup>	-17 ± 3 <sup>[c]</sup>
<b>3</b>	--	--	--	106.1 ± 1.1 <sup>[c]</sup>	61.7 ± 1.6 <sup>[c]</sup>	-149 ± 14 <sup>[c]</sup>
<b>4</b>	--	--	--	110.5 ± 1.6 <sup>[c]</sup>	86.7 ± 2.0 <sup>[c]</sup>	-80 ± 5 <sup>[c]</sup>

[a] In the gas phase (gas). [b] In the stationary phase (stat). [c] In the gas and stationary phase (app).

enantiomerization process (Scheme 3). The increase in the negative entropy  $\Delta S^{\ddagger}$  is characteristic for charge separation in heterolytic processes,<sup>[11a,12]</sup> but not for homolytic processes.<sup>[13]</sup>

For a heterolytic process, a mechanism via a thermally favored conrotatory electrocyclic ring opening–ring closing can be envisaged, as proposed for oxiranes and aziridines by Huisgen et al.<sup>[12b]</sup> The intermediate of the conrotatory electrocyclic ring opening in Scheme 3 shows charge separation and can be considered to be a heteroallyl anion with a considerable resonance energy.

## Experimental Section

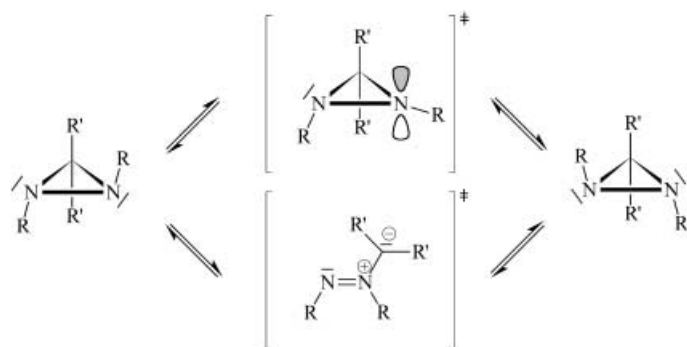
**1,2-Di-*tert*-butyldiaziridine (**1**):** This was prepared according to the method of Kostyanovsky et al.<sup>[21]</sup> *N*-Methylene-*tert*-butylamine (42.5 g, 0.5 mol), *tert*-butylamine (106 mL, 1.0 mol), and *tert*-butylhypochlorite (54 g, 0.5 mol) were dissolved in anhydrous diethyl ether (120 mL) in a 500 mL flask equipped with a magnetic stirrer and a drying tube. After stirring for six days at room temperature, the mixture was filtrated, and heated with solid KOH for 2 h. Diaziridine **1** was obtained as a colourless liquid after distillation under reduced pressure in 11.5% (9.0 g) yield. B.p. 40–42 °C (22 mbar); <sup>1</sup>H NMR (250 MHz, CDCl<sub>3</sub>, 25 °C, TMS):  $\delta$  = 0.96 (s, 18H, C(CH<sub>3</sub>)<sub>3</sub>), 2.29 ppm (s, 2H, N-CH<sub>2</sub>-N); <sup>13</sup>C NMR (63 MHz, CDCl<sub>3</sub>):  $\delta$  = 26.0 (CH<sub>3</sub>), 41.9 (C-N), 54.4 ppm (N-CH<sub>2</sub>-N); MS (EI, 200 °C, 70 eV): *m/z* (%): 156 (7) [M]<sup>+</sup>, 141 (1), 100 (15), 85 (10), 70 (10), 57 (100), 45 (12), 44 (11), 41 (10), 29 (8).

**1,2-Di-*n*-butyldiaziridine (**2**):** This was prepared according to the method of Ohme et al.<sup>[11g]</sup> *n*-butylamine (100 mL, 1 mol) and 2*N* NaOH (250 mL) were combined in a 1 L flask equipped with a magnetic stirrer and cooled to -20 °C. First concentrated formaldehyde solution (50 mL, 36% w/w) and then sodium hypochlorite solution (300 mL, 13% w/w) were added dropwise. The mixture was stirred at room temperature for 13 h, then the organic layer was separated and washed with diluted sodium thiosulfate solution and water. After the mixture was dried over KOH, filtered, and distilled under reduced pressure, **2** was obtained as a colorless liquid in 72.0% (56.0 g) yield. B.p. 34–36 °C (15 mbar); <sup>1</sup>H NMR (400 MHz, CDCl<sub>3</sub>):  $\delta$  = 0.92 (t, 6H; Me), 1.38 (qt, <sup>3</sup>J(H,H) = 7.0 Hz and 7.3 Hz, 4H, CH<sub>2</sub>Me), 1.57 (tdd, <sup>3</sup>J(H,H) = 7.3 Hz, 7.0 Hz and 7.9 Hz, 4H, CH<sub>2</sub>Et), 2.35 (m, 4H, CH<sub>2</sub>-N), 2.43 ppm (s, 2H, N-CH<sub>2</sub>-N); <sup>13</sup>C NMR (63 MHz, CDCl<sub>3</sub>):  $\delta$  = 13.16 (CH<sub>3</sub>), 19.69, 30.04 (CH<sub>2</sub>), 48.17 (CH<sub>2</sub>N), 55.77 ppm (N-CH<sub>2</sub>-N).

1-*n*-Butyl-3,3-dimethyl-diaziridine (**3**) and 1,2,3,3-tetramethyldiaziridine (**4**) were prepared as previously described.<sup>[1c,e,g]</sup>

**Enantioselective stopped-flow multidimensional gas chromatography (sfMDGC):** Enantioselective stopped-flow MDGC was performed on a Siemens Sichromat2 gas chromatograph equipped with two ovens, a pneumatically controlled six-port valve (Valco), a cooling trap in oven 2 for use with liquid nitrogen, two flame-ionization detectors and a Shimadzu C-R6A integrator. The whole process was monitored by a control computer.

For the separation of enantiomers of **1**, a fused silica column coated with Chiral- $\beta$ -Dex<sup>[5]</sup> (12.5 m × 0.25 mm i.d., 0.4  $\mu$ m film thickness, 80 °C, 0.5 bar column head pressure) in oven 1 was employed. Either the first or second eluted (pure) enantiomer of **1** was trapped in the reactor column,



Scheme 3. Possible enantiomerization pathways of diaziridines via two-fold nitrogen inversion or thermally favored conrotatory electrocyclic ring opening–ring closing mechanism.

a deactivated fused silica column coated with dimethylpolysiloxane (1 m × 0.25 mm i.d., 0.002 μm film thickness). The reactor column was quickly heated to temperature  $T$  whereby enantiomerization commenced. After the contact time  $t$ , the reactor column was rapidly cooled with liquid nitrogen and the de novo enantiomeric mixture was transferred at the separation temperature into the second separation column coated with Chirasil-β-Dex<sup>[5]</sup> (12.5 m × 0.25 mm i.d., 0.4 μm film thickness, 80 °C, 0.8 bar column head pressure at column 1), where the enantiomers were separated. Helium was used as the inert carrier gas. The experiment was repeated three times at each temperature. The enantiomerization rate constant in the gas phase  $k_1^{\text{gas}}$  was calculated from the observed de novo enantiomeric ratio (% *er*) of the major peak area, the temperature  $T$  and the contact time  $t$  according to Equation (2).

$$k_1^{\text{gas}} = \frac{1}{2t} \ln \frac{er + 1}{er - 1} \quad (2)$$

The mean values of  $\ln(k_{\text{gas}}/T)$  were plotted as a function of  $T^{-1}$  according to the Eyring equation. A linear fit was used to obtain  $\Delta H_{\text{gas}}^{\ddagger}$  and  $\Delta S_{\text{gas}}^{\ddagger}$  from the slope and the  $y$  intercept, respectively. A statistical factor  $\kappa$  of 0.5 for a reversible inversion process was applied.

**Enantioselective dynamic gas chromatography (DGC):** The enantiomeric separation of **1**, **2**, **3**, and **4** was performed on a Carlo Erba MEGA gas chromatograph, equipped with a liquid injector (250 °C), a flame-ionisation detector (250 °C) and a Shimadzu C-R 6A integrator and employed a fused silica column (50 m × 0.25 mm i.d.) coated with Chirasil-β-Dex<sup>[5]</sup> (0.3 μm film thickness). Dihydrogen was used as the carrier gas. The measurements were repeated at least three times at each temperature from 100.0–140.0 °C for **1**, 80.0–115.0 °C for **2**, 70.0–110 °C for **3** and 65.0–92.3 °C for **4**.

**Computer simulation:** The elution profiles obtained by DGC were evaluated with the ChromWin software,<sup>[11]</sup> specifically developed for the simulation of chromatographic elution profiles and the calculation of rate constants of reactions occurring on the partitioning time-scale. The experimentally determined chromatographic parameters, namely, the mobile phase hold-up time  $t_M$  (using methane), total retention times  $t_R$ , peak half-width  $\omega_h$ , peak heights  $h_A$  and  $h_B$  and the plateau height of the interconverting peaks  $h_{\text{plateau}}$  were used as input parameters for the simulation procedure. Peak form analysis was performed with the improved stochastic model (SM+) <sup>[11b]</sup> and “find enantiomerization barrier II” method in order to find the best agreement of the simulated and experimental elution profiles in only a few simulation steps, which yielded the apparent rate constants  $k_1^{\text{app}}$  and  $k_{-1}^{\text{app}}$  of enantiomerization in the presence of the chiral selectors whereby  $k_{-1}^{\text{app}}$  was calculated with Equations (1) from  $k_1^{\text{app}}$  according to the principle of microscopic reversibility.<sup>[7a]</sup>

To reduce the computation time, enantiomerization rate constants were calculated with the approximation function (AF)<sup>[10]</sup> and used as the starting point for the iterative simulation (in average only three steps were necessary).

## Acknowledgement

This work was supported by the Deutsche Forschungsgemeinschaft, Fonds der chemischen Industrie, and the Russian Foundation for Basic Research (grants DFG-RFBR 03-03-04010 and RFBR 03-03-32019). O.T. thanks the Deutsche Forschungsgemeinschaft (DFG) for an Emmy Noether Fellowship (TR 542/1-1).

- [1] a) A. Mannschreck, R. Radeaglia, E. Grundemann, R. Ohme, *Chem. Ber.* **1967**, *100*, 1778; b) A. Mannschreck, W. Seitz, *Angew. Chem.* **1969**, *81*, 224; *Angew. Chem. Int. Ed. Engl.* **1969**, *8*, 212; c) E. Haselbach, A. Mannschreck, W. Seitz, *Helv. Chim. Acta* **1973**, *56*, 156; d) H. Häkli, A. Mannschreck, *Angew. Chem.* **1977**, *89*, 419; *Angew. Chem. Int. Ed. Engl.* **1977**, *16*, 405; e) H. Häkli, M. Mintas, A. Mannschreck, *Chem. Ber.* **1979**, *112*, 2028; f) M. Mintas, A. Mannschreck, L. Klasinc, *Tetrahedron* **1981**, *37*, 867; g) R. Ohme, E. Schmitz, and P. Dolge, *Chem. Ber.* **1966**, *99*, 2104.
- [2] a) R. G. Kostyanovsky, A. E. Polyakov, V. I. Markov, *Izv. Akad. Nauk SSSR Ser. Khim.* **1974**, 1671 (in Russian); b) R. G. Kostyanovsky, A. E. Polyakov, G. V. Shustov, K. S. Zakharov, V. I. Markov, *Dokl. Akad. Nauk SSSR* **1974**, *219*, 873 (in Russian); c) R. G. Kostyanovsky, A. E. Polyakov, V. I. Markov, *Izv. Akad. Nauk SSSR Ser. Khim.* **1975**, 198 (in Russian); d) O. A. Dyachenko, L. O. Atovmyan, S. M. Aldoshin, A. E. Polyakov, *J. Chem. Soc. Chem. Commun.* **1976**, 50; e) R. G. Kostyanovsky, A. E. Polyakov, G. V. Shustov, *Tetrahedron Lett.* **1976**, 2059; f) G. V. Shustov, O. A. Dyachenko, S. M. Aldoshin, A. B. Zolotoi, M. D. Isobaev, I. I. Chervin, L. O. Atovmyan, R. G. Kostyanovsky, *Dokl. Akad. Nauk SSSR* **1976**, *231*, 1174 (in Russian); g) R. G. Kostyanovsky, V. F. Rudchenko, G. V. Shustov, *Izv. Akad. Nauk SSSR Ser. Khim.* **1975**, 198 (in Russian); h) R. G. Kostyanovsky, G. V. Shustov, A. I. Mischenko, V. I. Markov, *Izv. Akad. Nauk SSSR Ser. Khim.* **1976**, 2026 (in Russian); i) R. G. Kostyanovsky, V. F. Rudchenko, G. V. Shustov, *Izv. Akad. Nauk SSSR Ser. Khim.* **1977**, 1687 (in Russian); j) R. G. Kostyanovsky, G. V. Shustov, *Dokl. Akad. Nauk SSSR* **1977**, *232*, 1081 (in Russian); k) R. G. Kostyanovsky, G. V. Shustov, N. L. Zaichenko, *Tetrahedron* **1982**, *38*, 949; l) G. V. Shustov, A. B. Zolotoi, N. L. Zaichenko, O. A. Dyachenko, L. O. Atovmyan, R. G. Kostyanovsky, *Tetrahedron* **1984**, *40*, 2151; m) G. V. Shustov, S. N. Denisenko, M. A. Shochen, R. G. Kostyanovsky, *Izv. Akad. Nauk SSSR Ser. Khim.* **1988**, 1862 (in Russian); n) G. V. Shustov, A. Yu. Shibaev, Yu. V. Puzanov, R. G. Kostyanovsky, *Izv. Akad. Nauk SSSR Ser. Khim.* **1988**, 1869 (in Russian); o) G. V. Shustov, F. D. Polyak, V. S. Nosova, I. T. Liepinya, G. V. Nikiforovich, R. G. Kostyanovsky, *Khim. geterotsikl. Soedin.* **1988**, 1461 (in Russian); p) G. V. Shustov, G. K. Kadorkina, R. G. Kostyanovsky, A. Rauk, *J. Am. Chem. Soc.* **1988**, *110*, 1719; q) G. V. Shustov, G. K. Kadorkina, S. V. Varlamov, AV. Kachanov, R. G. Kostyanovsky, A. Rauk, *J. Am. Chem. Soc.* **1992**, *114*, 1616; r) R. G. Kostyanovsky, V. A. Korneev, I. I. Chervin, V. N. Voznesensky, Yu. V. Puzanov, P. Rademacher, *Mendeleev Commun.* **1996**, 106; s) N. N. Makhova, V. V. Kuznetsov, R. G. Kostyanovsky, *Izv. Akad. Nauk SSSR Ser. Khim.* **1996**, 1870.
- [3] W. B. Jennings, D. R. Boyd, in: *Cyclic Organonitrogen Stereodynamics* (Eds.: J. B. Lambert, Y. Takeuchi), VCH Publishers, New York, Weinheim, Cambridge **1992**, Chapt. 5, pp. 105–158.
- [4] a) R. G. Kostyanovsky, G. K. Kadorkina, V. R. Kostyanovsky, V. Schurig, O. Trapp, *Angew. Chem.* **2000**, *112*, 3066–3069; *Angew. Chem. Int. Ed.* **2000**, *39*, 2938; b) S. V. Usachev, G. N. Nikiforov, Yu. A. Strelenko, P. A. Belyakov, I. I. Chervin, R. G. Kostyanovsky, *Mendeleev Commun.* **2002**, 189; c) S. V. Usachev, G. N. Nikiforov, Yu. A. Strelenko, P. A. Belyakov, I. I. Chervin, K. A. Lyssenko, R. G. Kostyanovsky, *Mendeleev Commun.* **2003**, 136.
- [5] V. Schurig, D. Schmalzing, M. Schleimer, *Angew. Chem.* **1991**, *103*, 994; *Angew. Chem. Int. Ed. Engl.* **1991**, *30*, 987; H. Cousin, O. Trapp, V. Peulon-Agasse, X. Pannecoucke, L. Banspach, G. Trapp, Z. Jiang, J. C. Combret, V. Schurig, *Eur. J. Org. Chem.* **2003**, 3273–3287.
- [6] a) V. Schurig, S. Reich, *Chirality* **1998**, *10*, 316; S. Reich, V. Schurig, *J. Microcolumn Sep.* **1999**, *11*, 475; b) S. Reich, O. Trapp, V. Schurig, *J. Chromatogr. A* **2000**, *892*, 487; c) R. G. Kostyanovsky, V. Schurig,

- O. Trapp, K. A. Lyssenko, B. A. Averkiev, A. V. Prosyaniuk, G. K. Kadorkina, V. R. Kostyanovsky, *Mendeleev Commun.* **2002**, *12*, 137.
- [7] a) V. Schurig, W. Bürkle, A. Zlatkis, C. F. Poole, *Naturwissenschaften* **1979**, *66*, 423; b) W. Bürkle, H. Karfunkel, V. Schurig, *J. Chromatogr.* **1984**, *288*, 1; c) V. Schurig, M. Jung, M. Schleimer, F.-G. Klärner, *Chem. Ber.* **1992**, *125*, 1301; d) F. Gasparini, D. Misiti, M. Pierini, C. Villani, *Tetrahedron: Asymmetry* **1997**, *8*, 2069; e) J. Oxelbark, S. Allenmark, *J. Org. Chem.* **1999**, *64*, 1483; f) K. P. Scharwächter, D. H. Hochmuth, H. Dittmann, W. A. König, *Chirality* **2001**, *13*, 679; g) G. Schoetz, O. Trapp, V. Schurig, *Anal. Chem.* **2000**, *72*, 2758; h) G. Schoetz, O. Trapp, V. Schurig, *Anal. Chem.* **2000**, *72*, 2758; i) O. Trapp, V. Schurig, *Chem. Eur. J.* **2001**, *7*, 1495; j) O. Trapp, G. Schoetz, V. Schurig, *Chirality* **2001**, *13*, 403.
- [8] a) L. C. Craig, *J. Biol. Chem.* **1944**, *155*, 519; b) J. Kallen, E. Heilbronner, *Helv. Chim. Acta* **1960**, *43*, 489.
- [9] R. A. Keller, J. C. Giddings, *J. Chromatogr.* **1960**, *3*, 205.
- [10] a) O. Trapp, V. Schurig, *J. Chromatogr. A* **2001**, *911*, 167; b) O. Trapp, V. Schurig, *Chirality* **2002**, *14*, 465; c) O. Trapp, G. Trapp, J. Kong, U. Hahn, F. Vögtle, V. Schurig, *Chem. Eur. J.* **2002**, *8*, 3629; d) O. Trapp, G. Trapp, V. Schurig, *J. Biochem. Biophys. Methods* **2002**, *54*, 301.
- [11] a) O. Trapp, V. Schurig, *J. Am. Chem. Soc.* **2000**, *122*, 1424; b) O. Trapp, V. Schurig, *Comput. Chem.* **2001**, *25*, 187.
- [12] a) A. A. Frost, R. G. Pearson, *Kinetics Mechanism*, 2nd ed., Wiley, New York, **1961**, p. 135; b) H. Hermann, R. Huisgen, H. Mader, *J. Am. Chem. Soc.* **1971**, *93*, 1779; c) E. W. Yankee, F. D. Bader, N. E. Howe, D. J. Cram, *J. Am. Chem. Soc.* **1973**, *95*, 4210; d) O. Gonzales, D. E. Gallis, D. R. Crist, *J. Org. Chem.* **1986**, *51*, 3266; e) F. Gasparini, M. Pierini, C. Villani, D. Maria, A. Fontana, Ballini, *J. Org. Chem.* **2003**, *68*, 3173–3177.
- [13] a) H.-D. Beckhaus, G. Hellmann, C. Rüchardt, *Chem. Ber.* **1978**, *111*, 72; b) A. Haas, K. Schlosser, S. Steenken, *J. Am. Chem. Soc.* **1979**, *101*, 6282; c) K. Schlosser, S. Steenken, *J. Am. Chem. Soc.* **1983**, *105*, 1504.

Received: September 1, 2003 [F5494]